



# Liquid-like atoms in dense-packed solid glasses

C. Chang<sup>1,2,5</sup>, H. P. Zhang<sup>1,5</sup>, R. Zhao<sup>1,2,5</sup>, F. C. Li<sup>1</sup>, P. Luo<sup>1</sup>, M. Z. Li<sup>3</sup> and H. Y. Bai<sup>1,2,4</sup>✉

**Revealing the microscopic structural and dynamic pictures of glasses is a long-standing challenge for scientists<sup>1,2</sup>. Extensive studies on the structure and relaxation dynamics of glasses have constructed the current classical picture<sup>3–5</sup>: glasses consist of some ‘soft zones’ of loosely bound atoms embedded in a tightly bound atomic matrix. Recent experiments have found an additional fast process in the relaxation spectra<sup>6–9</sup>, but the underlying physics of this process remains unclear. Here, combining extensive dynamic experiments and computer simulations, we reveal that this fast relaxation is associated with string-like diffusion of liquid-like atoms, which are inherited from the high-temperature liquids. Even at room temperature, some atoms in dense-packed metallic glasses can diffuse just as easily as they would in liquid states, with an experimentally determined viscosity as low as  $10^7$  Pa·s. This finding extends our current microscopic picture of glass solids and might help establish the dynamics–property relationship of glasses<sup>4</sup>.**

Matter can generally be classified into solid, liquid and gas states. Under extreme conditions or in specific systems, special states of matter exist that simultaneously exhibit some properties of both liquid and solid. In this case, solid matter contains rapidly diffusing, liquid-like atoms that can move fast even at low temperatures. Although it seems incredible, the existence of rapidly diffusing, liquid-like atoms in solids has been reported many times. For example, it is presumed that solid  $^4\text{He}$  is able to enter a supersolid state in which  $^4\text{He}$  atoms can move fast and freely without any resistance<sup>10</sup>. In addition, a superionic state in which small/light atoms can diffuse freely while large/heavy atoms are fixed in their sublattices<sup>11–14</sup> has also been observed in materials, including ices<sup>11</sup>, helium–water compounds<sup>12</sup>, copper-based thermoelectric materials<sup>13</sup> and lithium-based conductors<sup>14</sup>, attracting growing attention in both materials science and engineering.

Because glassy solids are generally recognized to be frozen liquids<sup>2,4,5</sup>, it is reasonable to imagine that there are more possibilities to find rapidly diffusing liquid-like atoms in glasses. In fact, a previous study of amorphous  $\text{SiO}_2$  has even imaged liquid-like fast atoms at the edge of a two-dimensional sheet<sup>15</sup>. However, this fast motion was not ascribed to the amorphous nature but to the chemical-bond hierarchy<sup>15</sup>. Liquid-like atoms have rarely been observed in simple glasses, such as dense-packed metallic glasses (MGs). Recently, an unusual fast-relaxation process was observed in the dynamics of MGs at low temperatures where  $\alpha$  and  $\beta$  relaxations are too slow to be tracked<sup>6–9</sup>. This process was regarded as the precursor of  $\beta$  relaxation with more localized atomic motion, probably related to certain chemical bonds, and as the initiation of plasticity in MGs. However, the underlying mechanism of this fast relaxation has yet to be elucidated. It is unclear whether such a fast relaxation in glasses is related to the liquid-like atoms. Answers to these questions may change our basic understanding of glasses.

In this study we found that the fast relaxation in glasses is a continuation of the dynamics of high-temperature liquids, and its carriers are rapidly diffusing, liquid-like atoms inherited from high-temperature liquids. At room temperature (r.t.), these liquid-like atoms can diffuse rapidly with a viscosity as low as  $10^7$  Pa·s, which is six orders of magnitude lower than that of glasses ( $10^{13}$  Pa·s) at the glass transition temperature ( $T_g$ ). Molecular dynamics (MD) simulations reveal that this fast relaxation arises from string-like diffusion of the liquid-like atoms in MGs. These findings not only clarify the mechanism of fast relaxation, but also reveal deeper insights into the nature of glasses and the glass transition.

The initial clue to the existence of rapidly diffusing, liquid-like atoms in MGs comes from dynamics rather than from atomic structures. In fact, although current technology can capture the three-dimensional atomic structure of MGs<sup>16</sup>, it is still difficult to image the atomic motions in MGs. Dynamic spectra can provide a powerful tool to probe the features and basic properties of glasses<sup>4–6,17,18</sup>. Figure 1 shows the temperature-dependent loss modulus spectra of several typical MGs, where all samples exhibit three well-separated relaxation processes. Figure 1a shows that in  $\text{Al}_{85}\text{La}_{10}\text{Ni}_5$  MG, besides the  $\alpha$  relaxation, a  $\beta$ -relaxation hump at about 470 K ( $\sim 0.83T_g$ ) and a distinct peak at a lower temperature of 270 K ( $\sim 0.48T_g$ ) occur, indicating that there are some atoms moving much faster than atoms involved in  $\beta$  relaxation. Combining our results and previous reports<sup>6–9</sup>, it can be concluded that this fast process is not restricted to a specific composition but is a common phenomenon in MGs.

Next, to prove that the atoms which carry fast relaxation at low temperatures are intrinsically liquid-like, the activation energies were systematically studied. The fast-relaxation activation energy can be obtained from Arrhenius fitting to the frequency-dependent relaxation peak<sup>17</sup>, as shown in Fig. 2a–c. The fast-relaxation activation energies for  $\text{Y}_{68.9}\text{Co}_{31.1}$ ,  $\text{Ce}_{70}\text{Cu}_{20}\text{Al}_{10}$  and  $\text{Al}_{90}\text{La}_{10}$  MGs are 0.60, 0.46 and 0.47 eV, respectively. We further investigated the activation energy of atoms in high-temperature liquids. It has been well established that liquid dynamics exhibits simple Arrhenius behaviour at high temperatures above a crossover temperature<sup>19–21</sup>. That is, the activation energy of liquid dynamics has a fixed value in high-temperature liquids<sup>1,19</sup>. For the  $\text{Y}_{68.9}\text{Co}_{31.1}$  alloy, the viscosities  $\eta$  were measured at high temperatures by electrostatic levitation<sup>21</sup>. For the  $\text{Ce}_{70}\text{Cu}_{20}\text{Al}_{10}$  alloy, the self-diffusion coefficients  $D$  at high temperatures were obtained by quasi-elastic neutron scattering<sup>22</sup>. Meanwhile, we performed MD simulations for high-temperature  $\text{Al}_{90}\text{La}_{10}$  liquids to calculate the self-diffusion coefficients. The Arrhenius fittings to  $\eta$  or  $D$  give accurate estimates of the activation energies of the atomic dynamics in liquids, which are 0.63, 0.47 and 0.41 eV for  $\text{Y}_{68.9}\text{Co}_{31.1}$ ,  $\text{Ce}_{70}\text{Cu}_{20}\text{Al}_{10}$  and  $\text{Al}_{90}\text{La}_{10}$ , respectively. It is striking that the activation energies of the atomic dynamics

<sup>1</sup>Institute of Physics, Chinese Academy of Sciences, Beijing, China. <sup>2</sup>Center of Materials Science and Optoelectronics Engineering, University of Chinese Academy of Sciences, Beijing, China. <sup>3</sup>Department of Physics, Renmin University of China, Beijing, China. <sup>4</sup>Songshan Lake Materials Laboratory, Dongguan, Guangdong, China. <sup>5</sup>These authors contributed equally: C. Chang, H. P. Zhang, R. Zhao. ✉e-mail: [hybai@iphy.ac.cn](mailto:hybai@iphy.ac.cn)

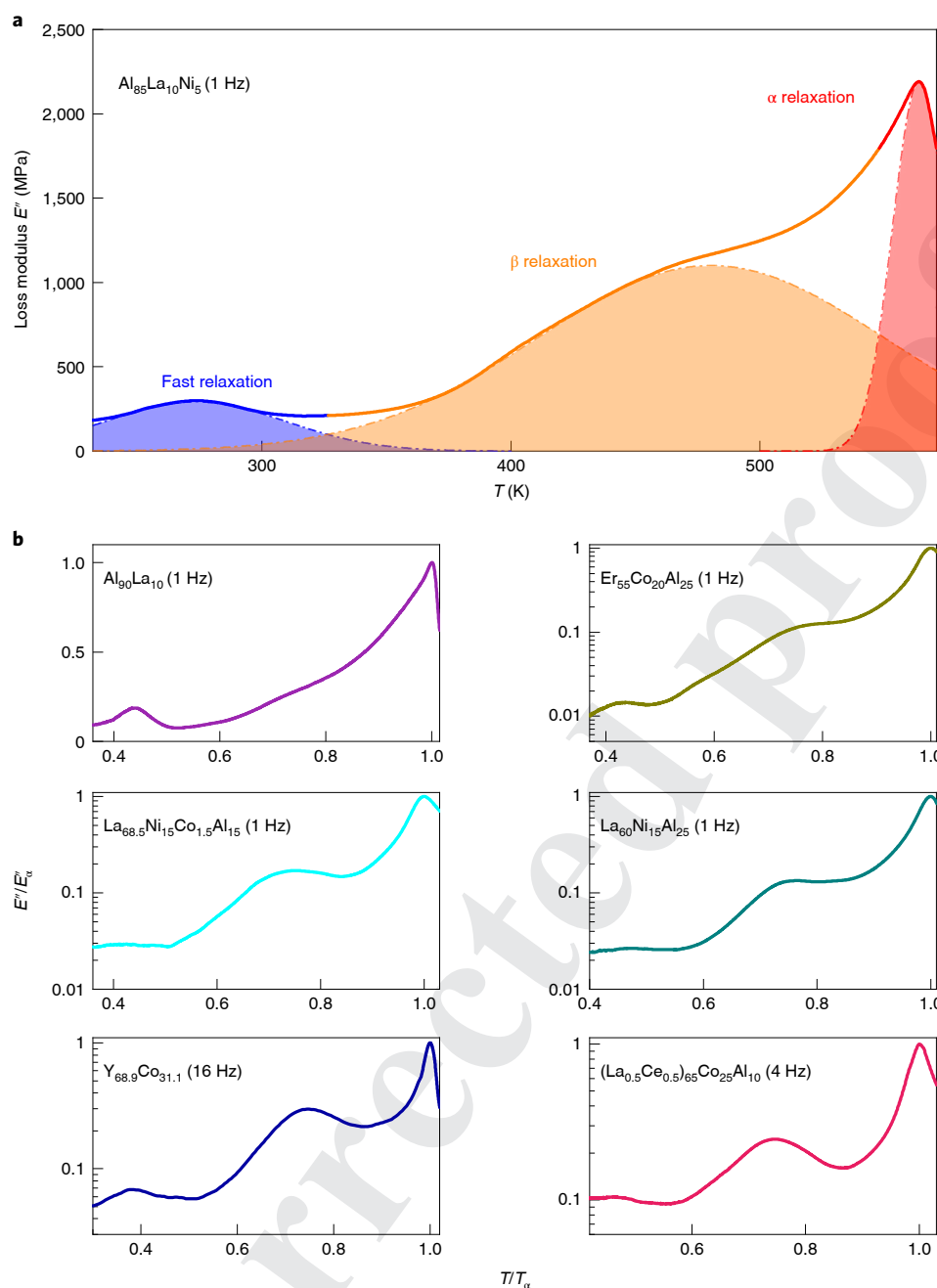


**Fig. 1 | Emergence of the fast-relaxation process in MGs on the dynamic mechanical spectra. a**, Loss modulus  $E''$  at a testing frequency of 1 Hz for  $\text{Al}_{85}\text{La}_{10}\text{Ni}_5$  MG, showing a distinct hump of  $\beta$  relaxation and a pronounced fast relaxation at temperatures far below that of  $\beta$  relaxation. The coloured regions provide a guide to the eye. **b**, Loss modulus  $E''$  for many other MGs, including  $\text{Al}_{90}\text{La}_{10}$ ,  $\text{Er}_{55}\text{Co}_{20}\text{Al}_{25}$ ,  $\text{La}_{68.5}\text{Ni}_{15}\text{Co}_{1.5}\text{Al}_{15}$ ,  $\text{La}_{60}\text{Ni}_{15}\text{Al}_{25}$ ,  $\text{Y}_{68.9}\text{Co}_{31.1}$  and  $(\text{La}_{0.5}\text{Ce}_{0.5})_{65}\text{Co}_{25}\text{Al}_{10}$ , showing a universal fast relaxation at low temperatures. Note that both  $\text{Al}_{85}\text{La}_{10}\text{Ni}_5$  and  $\text{Al}_{90}\text{La}_{10}$  show an obvious peak even in linear coordinates.

in high-temperature liquids and the fast relaxation in glasses are almost identical (Fig. 2a–c). Furthermore, we summarized the values of activation energies of  $\beta$  relaxation, fast relaxation and high-temperature liquid dynamics collected from the literature for various typical MGs<sup>6–8,17,21,23</sup>. As shown in Fig. 2d, the activation energies of fast relaxation and viscosity/diffusion of high-temperature liquids are quite close for different MGs, and an approximately linear relationship of activation energy  $\sim 12k_{\text{B}}T_{\text{g}}$  (where  $k_{\text{B}}$  is the Boltzmann constant) can be obtained, demonstrating an inherent correlation between the two processes.

In addition to the statistics of activation energy, we also compared the relaxation times of different dynamic processes in  $\text{Y}_{68.9}\text{Co}_{31.1}$ . The relaxation time  $\tau$  of a high-temperature liquid can be extracted from the viscosity  $\eta$  via the Maxwell relationship  $\eta = G_{\infty} \times \tau$ , where  $G_{\infty}$  is the instantaneous shear modulus. Figure 3 shows that the dynamics of a high-temperature liquid and fast relaxation collapses on a single master curve (the Arrhenius relation for liquids), revealing clearly the strong correlation between them and suggesting the inheritance of rapidly diffusing liquid-like atoms from high-temperature liquids into glass solids.

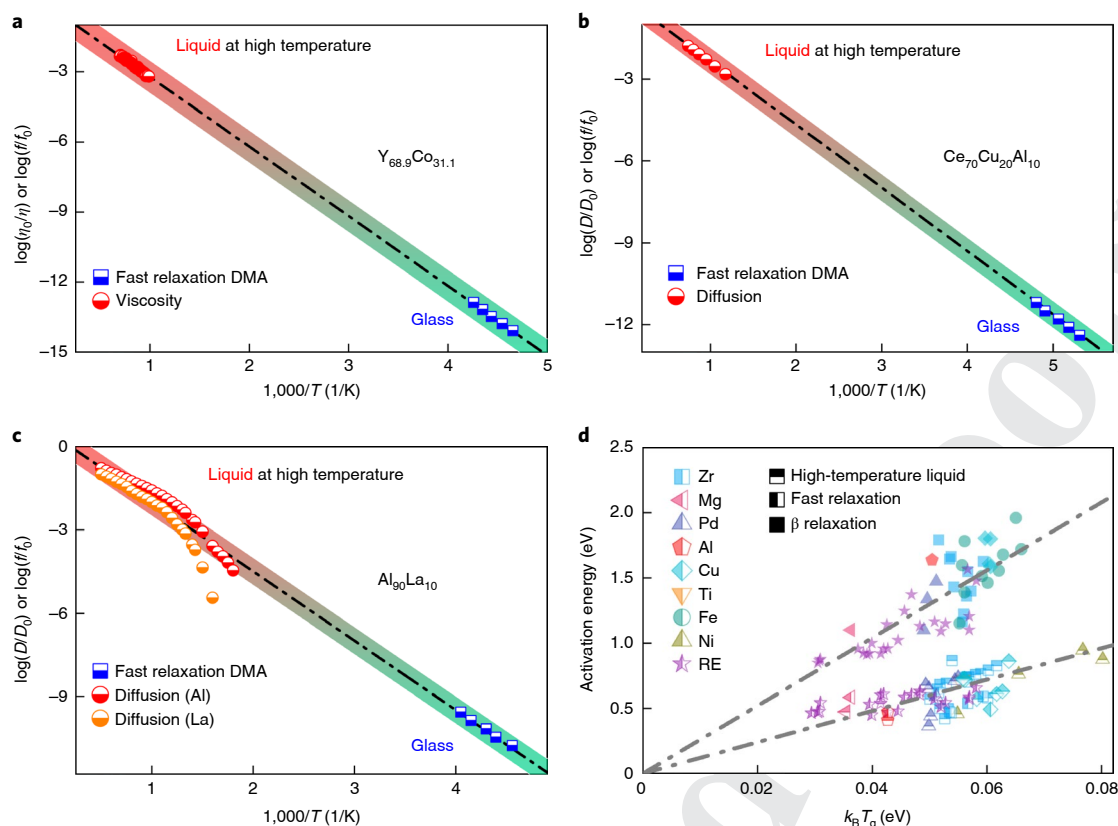


**Fig. 2 | Correlation between the activation energies of fast relaxation and high-temperature liquids.** **a**, The activation energy of fast relaxation of  $Y_{68.9}Co_{31.1}$  MG determined by DMA experiments and that of  $Y_{68.9}Co_{31.1}$  liquid obtained by viscosity measurement<sup>21</sup>. **b**, The activation energy of fast relaxation of  $Ce_{70}Cu_{20}Al_{10}$  MG determined by DMA experiments and that of self-diffusion of copper atoms in liquid  $Ce_{70}Cu_{20}Al_{10}$  derived from neutron scattering data<sup>22</sup>. **c**, The activation energy of fast relaxation of  $Al_{90}La_{10}$  MG determined by DMA experiments and that of liquid  $Al_{90}La_{10}$  calculated by MD simulations. **d**, Statistics of the activation energy of  $\beta$  relaxation (full-filling), fast relaxation (half-left-filling) and high-temperature liquid (half-up-filling) for a variety of MGs (different symbols), showing a close link between fast relaxation and high-temperature liquids. The data are listed in Supplementary Tables 1–3.

Previous studies have generally treated supercooled liquids as the parent phase of glass and ignored the possible inheritance from high-temperature liquids<sup>1,2,8,17,18</sup>. The finding of the inheritance of liquid-like atoms in glass from high-temperature liquids provides a very useful picture for glass structures and dynamics. Figure 3 shows that as temperature decreases, the dynamics of liquids deviates from Arrhenius behaviour, followed by subsequent decoupling of  $\alpha$  and  $\beta$  relaxations at the crossover temperature  $T_{\alpha\beta}$  in a moderately supercooled range<sup>1,17,18</sup>. Our results suggest an additional decoupling related to the fast relaxation at another crossover temperature. Many studies defined this crossover temperature as  $T_A$  and revealed that  $T_A$  is the onset temperature where flow starts to be microscopically cooperative<sup>20,21,24</sup>. Thus, this decoupling suggests that when the viscosity of a liquid deviates from Arrhenius behaviour, not all of the atoms take part in the cooperative flow; some atoms can maintain liquid Arrhenius behaviour even in glassy states, appearing as persistent liquid-like atoms. Similar decoupling was observed in a previous study of a polymer glass-forming system<sup>25</sup>, implying that the inheritance of liquid-like atoms might be a universal feature of disordered systems.

Next, we evaluated the viscosity of rapidly diffusing, liquid-like atoms at r.t. The motion of liquid-like atoms will cause an obvious anelastic hysteresis under superfast loading/unloading processes, which can be directly measured by nanoindentation experiments<sup>26</sup> (Supplementary Fig. 6). The viscosity of liquid-like atoms in the  $Y_{68.9}Co_{31.1}$  at r.t. was determined to be  $10^{6.93 \pm 0.02}$  Pa·s. According to our inheritance scenario, the viscosity of inherited liquid-like atoms at r.t. is estimated to be  $10^{6.44 \pm 0.02}$  Pa·s. The experimental viscosity

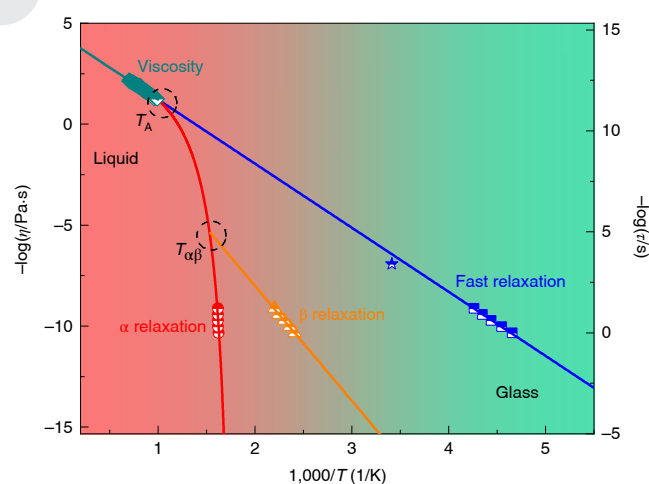


**Fig. 3 | Relaxation map from experimental results of a  $Y_{68.9}Co_{31.1}$  MG as a function of the inverse of temperature, illustrating how a deep glassy solid inherits liquid-like atoms from a high-temperature liquid.** The red line is the Vogel-Fulcher-Tammann<sup>1</sup> fit to the  $\alpha$ -relaxation data; the orange line is the Arrhenius fit to the  $\beta$ -relaxation data; the blue line is the Arrhenius fit to the fast-relaxation data, and the dark-green line is the Arrhenius fit to the viscosity data<sup>21</sup>. The half-filled blue star represents the measured viscosity at r.t. for liquid-like atoms via a nanoindentation experiment. The  $\alpha$ -relaxation,  $\beta$ -relaxation and fast-relaxation data are measured by DMA. The dotted circles represent crossover points  $T_{\alpha\beta}$  and  $T_A$ .

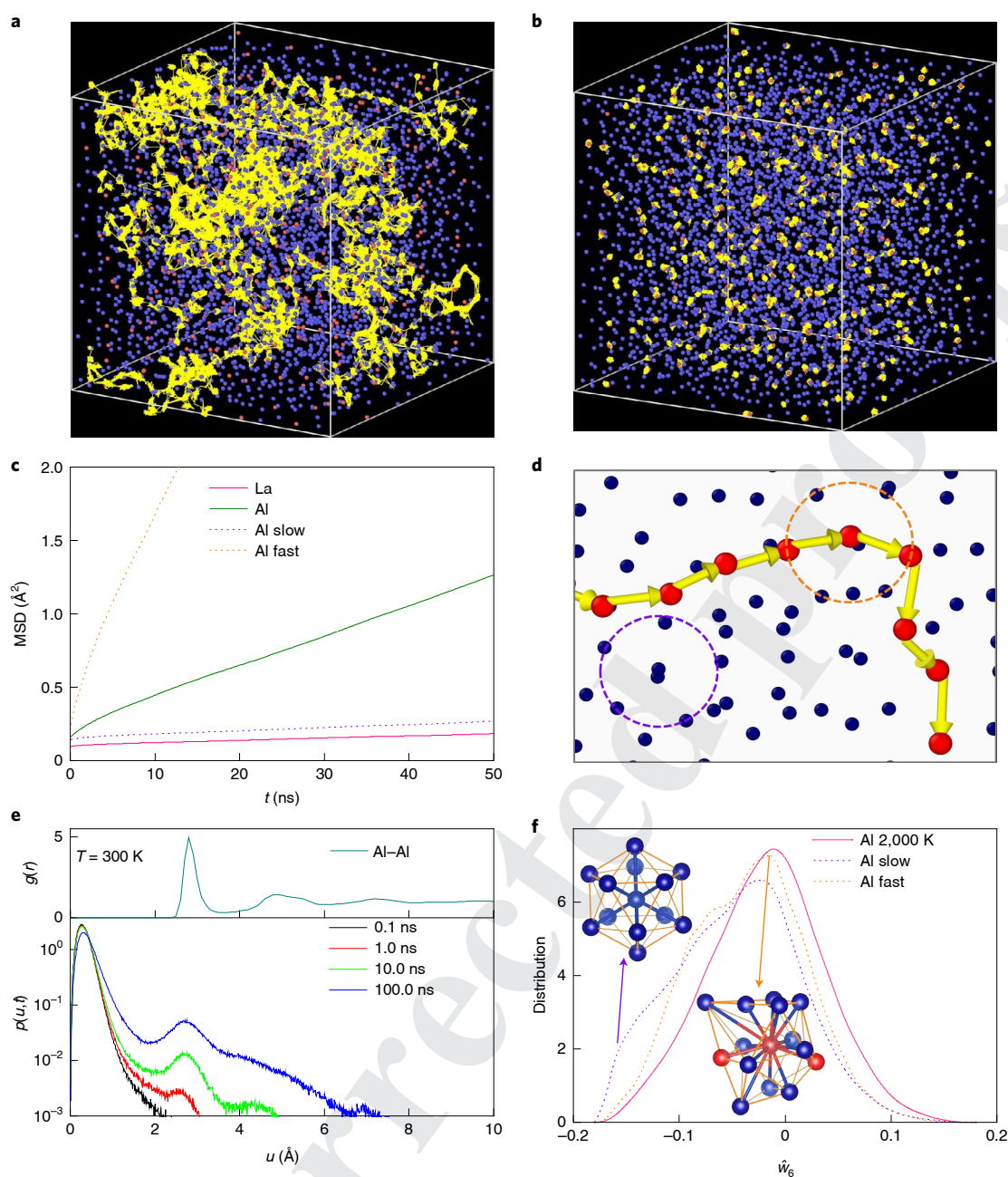


**Fig. 4 | Identification and characterization of liquid-like atoms in  $\text{Al}_{90}\text{La}_{10}$  MG at r.t. (300 K) by MD simulations.** **a, b**, Atomic trajectories (yellow lines) during 100 ns in MD simulations for aluminium (**a**) and lanthanum (**b**). The red and blue balls represent the initial positions of lanthanum and aluminium atoms, respectively. The trajectories in **a** are only shown for fast atoms that end up more than 2.0 Å away from their initial positions. **c**, MSDs for different atoms. **d**, The spatial distribution of the liquid-like atoms (red balls) and their atomic displacements (yellow arrows). The circles indicate the clusters shown in **f**. **e**, The atomic displacement distribution  $p(u,t)$  and the pair correlation function  $g(r)$ . **f**, The probability distribution for the bond-orientational order parameter  $\hat{w}_6$ . For comparison, the  $\hat{w}_6$  of aluminium atoms in high-temperature liquids (2,000 K) is also presented. Insets: an icosahedral cluster with high symmetry, and a low-symmetric cluster around fast-diffusive atoms marked in red. Both clusters are circled in **d**.

(Fig. 3, half-filled blue star) is close to the predicted value (Fig. 3, blue curve), confirming the inheritance scenario. As a comparison, a low viscosity of  $10^8 \text{ Pa}\cdot\text{s}$  for nanosized Pd–Si MGs has been reported<sup>27</sup>, revealing the liquid-like nature of MG nanoparticles. The viscosity for the atoms carrying fast relaxation here ( $10^7 \text{ Pa}\cdot\text{s}$ ) is even smaller than that in Pd–Si nanoparticles, implying that these atoms actually exhibit liquid behaviour.

Further, we performed extensive MD simulations on  $\text{Al}_{90}\text{La}_{10}$  MG with pronounced fast relaxation. Figure 4a,b plot the trajectories of aluminium and lanthanum atoms in  $\text{Al}_{90}\text{La}_{10}$  at 300 K during

100 ns simulations. All lanthanum atoms vibrate around their equilibrium positions. In contrast, some aluminium atoms can move out of their cages. The analysis of mean square displacements (MSDs) in Fig. 4c shows clearly that these fast aluminium atoms can diffuse as in liquid states, which is further confirmed by calculating the Lindeman parameter<sup>28,29</sup> (Supplementary Fig. 11).

Importantly, Fig. 4d shows that the motions of liquid-like atoms form string-like structures, suggesting that fast diffusion of liquid-like atoms in MGs is not random but cooperative<sup>30</sup>. The atomic displacements (Fig. 4e) display clear multi-peaks,



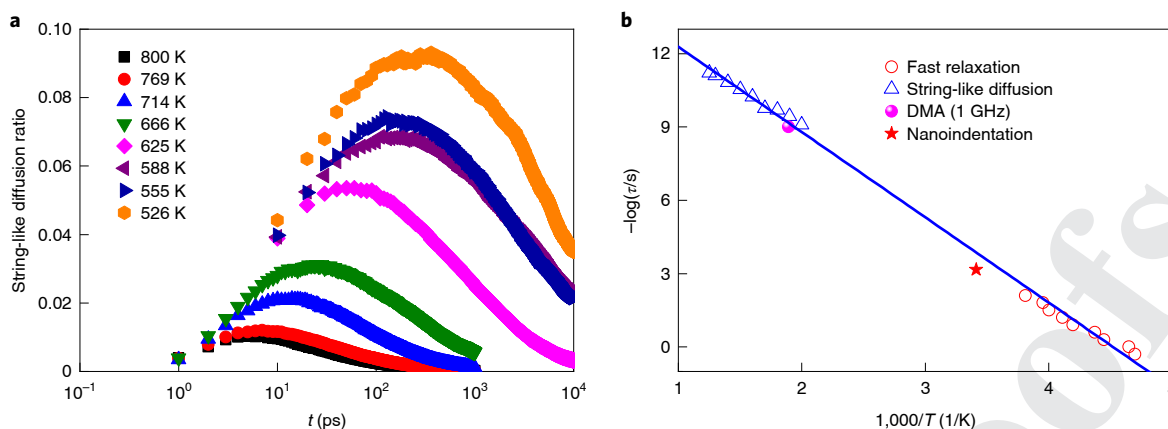


**Fig. 5 | Inheritance of string-like diffusion in the  $\text{Al}_{90}\text{La}_{10}$  system.** **a**, The ratio of atoms participating in string-like diffusion to the total number of fast-moving atoms versus time at different temperatures. **b**, The various relaxation times, including the string-like diffusion, the high-frequency DMA (1 GHz) testing in simulations, the measured fast relaxation in DMA experiments, and the superfast anelastic behaviour at r.t. measured by nanoindentation.

corresponding to the peaks in pair correlation functions. This confirms that the liquid-like atoms diffuse in a cooperative manner, that is, one atom jumps to the adjacent position that was previously occupied by another atom, generally one of its nearest neighbours. There is almost no difference between the atomic volumes of fast and slow aluminium atoms (Supplementary Fig. 12c). In contrast, the statistics of atomic-bond-orientational order parameter  $\psi_6$  (ref. <sup>31</sup>) in Fig. 4f shows that liquid-like atoms exist within more disordered environments and share more similarity with atoms in a liquid, implying that liquid-like atoms usually have lower-symmetric cages that are easier to break. When a neighbouring atom moves away, the centre atom simultaneously hops to this neighbouring site, and another neighbouring atom hops to the centre site at the same time, forming string-like structures (Fig. 4d).

Next, we investigated the inheritance process of liquid-like atoms. Because the liquid-like atoms diffuse in a string-like manner, we analysed the ratio of atoms participating in string-like diffusion to the total number of fast-moving atoms, from high-temperature liquids to glasses. The ratio in Fig. 5a shows clear peaks at all temperatures. As the temperature decreases, the peak shifts to longer times, indicating the slowing down of string-like diffusion. Meanwhile, the peak intensity increases strongly with decreasing temperature, implying that the string-like diffusion becomes increasingly pronounced. We hypothesize that most of the fast-moving atoms will participate in string-like diffusion at cryogenic temperatures, resulting in the fast relaxation. Furthermore, the relaxation time for string-like diffusion is calculated as the time when the ratio reaches its maximum. The relaxation time continues the Arrhenius relation of liquid (Fig. 5b), and its extension goes across the experimental dynamic mechanical analysis (DMA) data of fast relaxation. This provides strong evidence that the fast relaxation is caused by string-like diffusion inherited from the high-temperature liquid.

For further evidence, high-frequency DMA measurement at 1 GHz was performed via MD simulations. The loss modulus spectrum shows clearly two peaks at 665 and 528 K, respectively (Supplementary Fig. 13). The peak at 528 K was plotted as a magenta sphere in Fig. 5b, in agreement with the master curve of string-like diffusion. This provides direct evidence that the fast relaxation revealed by DMA experiments is associated with string-like diffusion. Nanoindentation was conducted to detect the rapidly diffusing, liquid-like atoms in  $\text{La}_{10}\text{Al}_{90}$  at r.t. It gives a relaxation time of 0.70 ms, which is consistent with that of string-like diffusion. Based on these experimental and simulated results, we concluded that the fast relaxation is the inherited motion from liquids.

The observation of liquid-like atoms in dense MGs deepens our understanding of the nature of glasses. Although a previous study of amorphous  $\text{SiO}_2$  imaged liquid-like fast atoms at the edge of a two-dimensional sheet<sup>15</sup>, the fast motion there was due to the chemical-bond hierarchy. The case in MGs is quite different. First, unlike oxide glasses, which have complex covalent network structures, MGs have simple atomic structures similar to the random packing of spheres that are unlikely to result in chemical-bond hierarchy<sup>18,32</sup>. Second, MGs are quite densely packed compared with  $\text{SiO}_2$  glass<sup>33</sup>. Therefore, the finding of rapidly diffusing, liquid-like atoms in dense-packed MGs reveals a more universal and extraordinary feature of glass solids: liquid-like atoms can be inherited from a high-temperature liquid into a glass during the glass formation, and a glassy solid is essentially part solid and part liquid.

The inheritance scenario demonstrated here challenges the previous understanding of fast relaxation. Fast relaxation has long been taken to be a more localized mode and a precursor of  $\beta$  relaxation<sup>6–8,34</sup>. Under this localized scenario, fast relaxation is related closely to  $\beta$  relaxation and is expected to evolve into  $\beta$  relaxation as in the transition from  $\beta$  to  $\alpha$  relaxation. However, this scenario is not supported by experimental results. On the one hand, according to a wide range of experimental results, the composition dependences of fast and  $\beta$  relaxations are quite irrelevant, that is, a system with pronounced fast relaxation does not necessarily exhibit pronounced  $\beta$  relaxation. On the other hand, fast relaxation will not merge into  $\beta$  relaxation but directly into the Arrhenius relation of liquid (Fig. 3). This is not observed exclusively in Y–Co but is a universal feature of various MGs (Supplementary Fig. 7). These facts suggest that fast relaxation is probably not a more localized motion or a precursor of  $\beta$  relaxation, but an inheritance of liquid dynamics demonstrated here. In contrast to the localized motion, the liquid-like atoms carrying fast relaxation may be located inside or outside the flow units of  $\beta$  relaxation. When these liquid-like atoms are activated, our simulation shows that they have clearly broken their low-symmetry cages and exhibit string-like cooperative diffusion. Unlike the  $\beta$  relaxation induced by local, loosely packed atoms, these liquid-like atoms are associated with an extremely disordered local structure.  $\beta$  relaxation is believed to be the inheritance from supercooled liquids, whereas fast relaxation is the inheritance of liquid-like atoms from high-temperature liquids.

The finding of liquid-like atoms in MGs provides more complete microcosmic structural and dynamic pictures of glasses, which can help understand the dynamics–property relationship in MGs. In this work, we confirm that the liquid-like atoms control the

superfast anelasticity of MGs at r.t., which is crucial for the application of MGs in microelectromechanical systems<sup>35</sup> and high-precision sensors<sup>36</sup>. The liquid-like atoms exist within highly disordered local environments which may act as defects to promote the formation of multiple shear bands and therefore increase the plasticity of MGs<sup>37</sup>. For example, recent studies reported a synchronously non-monotonic change between compression plasticity and fast relaxation in a high-entropy MG<sup>38</sup>. Meanwhile, the time scale of fast relaxation at r.t. is comparable with the frequency at which ultrasonic moulding can join MG ribbons together into bulk<sup>39</sup>, implying that liquid-like atoms play a role in the mechanism of cold-joining processes. In other systems these liquid-like atoms have also been found to influence thermal conductivity<sup>13,28</sup>, which helps design functional glasses.

In summary, by combining dynamic mechanical studies and detailed MD simulations, we demonstrate that the general fast dynamics of MGs at low temperatures is related to liquid-like atoms in glass solids. The liquid-like atoms are inherited from high-temperature liquids and exhibit behaviour similar to that in liquids, including comparable activation energies and low viscosities of  $\sim 10^7$  Pa·s at r.t. These findings extend our current understanding of the microscopic structural and dynamic pictures of glasses and have implications for establishing the dynamics–property relationship in glasses.

### Online content

Any methods, additional references, Nature Research reporting summaries, source data, extended data, supplementary information, acknowledgements, peer review information; details of author contributions and competing interests; and statements of data and code availability are available at <https://doi.org/10.1038/s41563-022-01327-w>.

Received: 10 November 2021; Accepted: 30 June 2022;

### References

1. Debenedetti, P. G. & Stillinger, F. H. Supercooled liquids and the glass transition. *Nature* **410**, 259–267 (2001).
2. Berthier, L. & Biroli, G. Theoretical perspective on the glass transition and amorphous materials. *Rev. Mod. Phys.* **83**, 587–645 (2011).
3. Wagner, H. et al. Local elastic properties of a metallic glass. *Nat. Mater.* **10**, 439–442 (2011).
4. Wang, W. H. Dynamic relaxations and relaxation–property relationships in metallic glasses. *Prog. Mater. Sci.* **106**, 100561 (2019).
5. Wang, Z., Sun, B. A., Bai, H. Y. & Wang, W. H. Evolution of hidden localized flow during glass-to-liquid transition in metallic glass. *Nat. Commun.* **5**, 5823 (2014).
6. Wang, Q. et al. Unusual fast secondary relaxation in metallic glass. *Nat. Commun.* **6**, 7876 (2015).
7. Zhao, L. Z. et al. A fast dynamic mode in rare earth based glasses. *J. Chem. Phys.* **144**, 204507 (2016).
8. Wang, Q. et al. Universal secondary relaxation and unusual brittle-to-ductile transition in metallic glasses. *Mater. Today* **20**, 293–300 (2017).
9. Küchemann, S. & Maaß, R. Gamma relaxation in bulk metallic glasses. *Scr. Mater.* **137**, 5–8 (2017).
10. Day, J. & Beamish, J. Low-temperature shear modulus changes in solid <sup>4</sup>He and connection to supersolidity. *Nature* **450**, 853–856 (2007).
11. Cavazzoni, C. et al. Superionic and metallic states of water and ammonia at giant planet conditions. *Science* **283**, 44–46 (1999).

12. Liu, C. et al. Multiple superionic states in helium–water compounds. *Nat. Phys.* **15**, 1065–1070 (2019).
13. Liu, H. L. et al. Copper ion liquid-like thermoelectrics. *Nat. Mater.* **11**, 422–425 (2012).
14. Wang, Y. et al. Design principles for solid-state lithium superionic conductors. *Nat. Mater.* **14**, 1026–1031 (2015).
15. Huang, P. Y. et al. Imaging atomic rearrangements in two-dimensional silica glass: watching silica's dance. *Science* **342**, 224–227 (2013).
16. Yang, Y. et al. Determining the three-dimensional atomic structure of an amorphous solid. *Nature* **592**, 60–64 (2021).
17. Yu, H. B., Wang, W. H., Bai, H. Y. & Samwer, K. The  $\beta$ -relaxation in metallic glasses. *Nat. Sci. Rev.* **1**, 429–461 (2014).
18. Luo, P., Wen, P., Bai, H. Y., Ruta, B. & Wang, W. H. Relaxation decoupling in metallic glasses at low temperatures. *Phys. Rev. Lett.* **118**, 225901 (2017).
19. Angell, C. A. Formation of glasses from liquids and biopolymers. *Science* **267**, 1924–1935 (1995).
20. Iwashita, T., Nicholson, D. M. & Egami, T. Elementary excitations and crossover phenomenon in liquids. *Phys. Rev. Lett.* **110**, 205504 (2013).
21. Blodgett, M. E., Egami, T., Nussinov, Z. & Kelton, K. F. Proposal for universality in the viscosity of metallic liquids. *Sci. Rep.* **5**, 13837 (2015).
22. Chathoth, S. M., Damaschke, B., Embs, J. P. & Samwer, K. Giant changes in atomic dynamics on microalloying metallic melt. *Appl. Phys. Lett.* **95**, 191907 (2009).
23. Yu, H. B., Wang, W. H., Bai, H. Y., Wu, Y. & Chen, M. W. Relating activation of shear transformation zones to beta relaxations in metallic glasses. *Phys. Rev. B* **81**, 4 (2010).
24. Pueblo, C. E., Sun, M. & Kelton, K. F. Strength of the repulsive part of the interatomic potential determines fragility in metallic liquids. *Nat. Mater.* **16**, 792–796 (2017).
25. Beiner, M. & Ngai, K. L. Interrelation between primary and secondary relaxations in polymerizing systems based on epoxy resins. *Macromolecules* **38**, 7033–7042 (2005).
26. Huo, L. S., Zeng, J. F., Wang, W. H., Liu, C. T. & Yang, Y. The dependence of shear modulus on dynamic relaxation and evolution of local structural heterogeneity in a metallic glass. *Acta Mater.* **61**, 4329–4338 (2013).
27. Cao, C. R. et al. Liquid-like behaviours of metallic glassy nanoparticles at room temperature. *Nat. Commun.* **10**, 1966 (2019).
28. Qiu, W. J. et al. Part-crystalline part-liquid state and rattling-like thermal damping in materials with chemical-bond hierarchy. *Proc. Natl Acad. Sci. USA* **111**, 15031–15035 (2014).
29. Lindemann, F. A. The calculation of molecular eigen-frequencies. *Phys. Z.* **11**, 609–612 (1910).
30. Zhang, H., Wang, X., Yu, H. B. & Douglas, J. F. Fast dynamics in a model metallic glass-forming material. *J. Chem. Phys.* **154**, 084505 (2021).
31. Nelson, D. R. Order, frustration, and defects in liquids and glasses. *Phys. Rev. B* **28**, 5515–5535 (1983).
32. Miracle, D. B. A structural model for metallic glasses. *Nat. Mater.* **3**, 697–702 (2004).
33. Rouxel, T., Ji, H., Hammouda, T. & Moreac, A. Poisson's ratio and the densification of glass under high pressure. *Phys. Rev. Lett.* **100**, 4 (2008).
34. Fan, Y., Iwashita, T. & Egami, T. How thermally activated deformation starts in metallic glass. *Nat. Commun.* **5**, 5083 (2014).
35. Middlemiss, R. P. et al. Measurement of the Earth tides with a MEMS gravimeter. *Nature* **531**, 614–617 (2016).
36. Ghadimi, A. H. et al. Elastic strain engineering for ultralow mechanical dissipation. *Science* **360**, aar6939 (2018).
37. Ma, E. Tuning order in disorder. *Nat. Mater.* **14**, 547–552 (2015).
38. Wu, Y. et al. Substantially enhanced plasticity of bulk metallic glasses by densifying local atomic packing. *Nat. Commun.* **12**, 6582 (2021).
39. Ma, J. et al. Fast surface dynamics enabled cold joining of metallic glasses. *Sci. Adv.* **5**, eaax7256 (2019).

**Publisher's note** Springer Nature remains neutral with regard to jurisdictional claims in published maps and institutional affiliations.

© The Author(s), under exclusive licence to Springer Nature Limited 2022

## Methods

**Material preparation.** The MG-forming alloy ingots with various nominal compositions were prepared by arc-melting mixtures of pure metals in a titanium-gettered argon atmosphere. Each ingot was melted at least five times to ensure chemical homogeneity. Eventually, glassy ribbons with thickness of about 30  $\mu\text{m}$  were fabricated by the single-roll melt-spining in an argon atmosphere. The amorphous nature of the samples was verified by the X-ray diffraction using Cu K $\alpha$  radiation (Supplementary Fig. 1).

**DMA.** The relaxation behaviours of selected MGs were characterized by a TA Q800 dynamic mechanical analyser. The dynamic modulus  $E^*(\omega) = E'(\omega) + iE''(\omega)$ , where the real part  $E'$  and imaginary part  $E''$  represent the storage and loss modulus, respectively, was measured in film tension mode with a constant heating rate of 3 K  $\text{min}^{-1}$  and different single testing frequencies or discrete frequencies of 1, 2, 4, 8 and 16 Hz (Supplementary Figs. 2–4).

**Nanoindentation.** Nanoindentation was performed on a TI 980 TriboIndenter system with a 5  $\mu\text{m}$  spherical indenter at r.t. (293 K). The peak loads of  $\text{Al}_{90}\text{La}_{10}$  and  $\text{Y}_{68.9}\text{Co}_{31.1}$  were set to 500 and 200  $\mu\text{N}$ , respectively; and the fast-loading times of  $\text{Al}_{90}\text{La}_{10}$  and  $\text{Y}_{68.9}\text{Co}_{31.1}$  were set to 0.005 and 0.01 s, respectively. In all of these tests, the slow-loading, holding and unloading time were both fixed at 0.1 s (Supplementary Figs. 5 and 6).

**MD simulation.** MD simulations were conducted within the LAMMPS software package to prepare and analyse  $\text{Al}_{90}\text{La}_{10}$  alloy using the embedded atom method potentials. In MD simulations, each sample contains 4,000 atoms in a cubic box with periodic boundary conditions applied in three directions. The samples were first equilibrated at 2,000 K for 2.0 ns, followed by hyperquenching to 100 K with cooling rate of  $1.0 \times 10^{12} \text{ K s}^{-1}$ , and further relaxed at 100 K for 2.0 ns (Supplementary Fig. 8). A time step of 2.0 fs was selected. The quenching process was performed in the NPT ensemble with zero pressure. The quenched sample was further relaxed at different temperatures in the NVT ensemble for statistics and analysis. More details about the simulation and calculations can be found in the Supplementary Information.

**Calculation of self-diffusion coefficient  $D$ .** The self-diffusion coefficient  $D$  in liquids was calculated via linear fitting of the long-time MSD at different temperatures. The MSD is defined as  $\Delta r^2(t) = N^{-1} \sum_{j=1}^N \langle (\mathbf{r}_{j,t} - \mathbf{r}_{j,0})^2 \rangle$ , where  $N$  is the number of atoms, and  $\mathbf{r}_{j,0}$  and  $\mathbf{r}_{j,t}$  represent the coordinate vector of atom  $j$  at zero and time  $t$ , respectively. The self-diffusion coefficient  $D$  can be calculated as  $D = \lim_{t \rightarrow \infty} \frac{\Delta r^2(t)}{6t}$ . More details can be found in Supplementary Fig. 9.

**Atomic volume and bond-orientational order parameters.** To characterize the local atomic structures, Voronoi tessellation was used to divide space into close-packed polyhedra around atoms by constructing bisecting planes along the lines joining the central atom and all of its neighbours. The volume of the Voronoi polyhedral surrounding each atom is calculated as the atomic volume  $V_a$ . To quantitatively describe the bond-orientational symmetry around the central atom, the bond-orientational order (BOO) parameters were employed via spherical harmonic expansion. Specifically, the BOO of atom  $i$  can be represented by the  $l$ -fold symmetry as a  $2l+1$  vector defined as  $q_{lm}(i) = \frac{1}{N_i} \sum_{j=1}^{N_i} Y_{lm}(\theta(\mathbf{r}_{ij}), \phi(\mathbf{r}_{ij}))$ , where  $Y_{lm}$  are spherical harmonics and  $N_i$  is the number of nearest neighbours (Voronoi neighbours in our case) around atom  $i$ . The rotational invariants for atom  $i$  can be defined as  $q_l = \sqrt{\frac{4\pi}{2l+1} \sum_{m=-l}^l |q_{lm}|^2}$  and  $w_l = \sum \begin{pmatrix} l & l & l \\ m_1 & m_2 & m_3 \end{pmatrix} \cdot q_{lm_1} \cdot q_{lm_2} \cdot q_{lm_3}$ . Here the term in brackets is the Wigner 3- $j$  symbol. Instead of  $w_l$ , the normalized parameter defined as

$\hat{w}_l = w_l \cdot \left( \sum_{m=-l}^l |q_{lm}|^2 \right)^{-3/2}$  is a more sensitive measure of the different orientational symmetries and is often used to evaluate the BOO. For example, the  $\hat{w}_6$  values of face-centred cubic, hexagonal close-packed and icosahedron clusters are  $-0.01316$ ,  $-0.01244$  and  $-0.16975$ , respectively.

**Ratio of string-like diffusion.** Here we define the atom  $j$  as a fast-moving atom if it moves more than 2.0  $\text{\AA}$  during a time interval  $t$  ( $|\mathbf{r}_{j,t} - \mathbf{r}_{j,0}| > 2.0 \text{ \AA}$ ). And define the atom  $j$  as a string-like atom if it moves to the original position of another atom ( $|\mathbf{r}_{j,t} - \mathbf{r}_{k,0}| < 0.3 \text{ \AA}$ ). We count the total number of fast-moving atoms ( $N_{\text{fast}}$ ) and number of string-like atoms ( $N_{\text{string}}$ ), and use their ratio ( $N_{\text{string}}/N_{\text{fast}}$ ) to describe the intensity of string-like diffusion.

**High-frequency DMA testing.** To prove that fast relaxation does exist in the high-temperature liquid, we also performed high-frequency DMA testing via MD simulations. A sinusoidal strain  $\epsilon(t) = \epsilon_A \sin(2\pi f_A t)$  was applied to the samples along the  $x$ - $y$  direction, where  $f_A$  is the frequency and selected as 1 GHz, and  $\epsilon_A$  is fixed at 1%. For statistics, 100 independent sinusoidal shear deformation simulations were performed at each temperature. For each MD-DMS loading, ten cycles were used. We fitted the stress as  $\sigma(t) = \sigma_0 + \sigma_A \sin(2\pi f_A t + \delta)$ , where  $\sigma_0$  is a constant term and  $\delta$  is the phase difference between stress and strain. Loss moduli are calculated according to  $E'' = \sigma_A/\epsilon_A \sin(\delta)$  (Supplementary Fig. 13).

## Data availability

The data supporting the findings of this work are included within the paper and its Supplementary Information files. Extra data are available from the corresponding authors upon reasonable request.

## Acknowledgements

This work was supported by the National Natural Science Foundation of China (grant numbers 52192600 (H.Y.B.), 61888102 (H.Y.B.), 11790291 (H.Y.B.), 52031016 (M.Z.L.), 51631003 (M.Z.L.)), the Natural Science Foundation of Guangdong Province (2019B030302010 (H.Y.B.)), the Strategic Priority Research Program of the Chinese Academy of Sciences (XDB30000000 (H.Y.B.)), the National Key Research and Development Plan (2018YFA0703603 (H.Y.B.)) and the China Postdoctoral Science Foundation (2020TQ0346 (F.C.L.), 2021M693372 (H.P.Z.)). We thank W. H. Wang for discussions.

## Author contributions

H.Y.B., M.Z.L. and R.Z. conceived the idea and designed the research. C.C. and R.Z. prepared the samples and conducted the DMA experiments. C.C. and F.C.L. performed the nanoindentation experiments. H.P.Z. and M.Z.L. performed numerical simulations. All authors analysed and reviewed the results, and participated in writing the paper. H.Y.B. supervised the project.

## Competing interests

The authors declare no competing interests.

## Additional information

**Supplementary information** The online version contains supplementary material available at <https://doi.org/10.1038/s41563-022-01327-w>.

**Correspondence and requests for materials** should be addressed to H. Y. Bai.

**Peer review information** *Nature Materials* thanks the anonymous reviewers for their contribution to the peer review of this work.

**Reprints and permissions information** is available at [www.nature.com/reprints](http://www.nature.com/reprints).

# QUERY FORM

| Nature Materials     |                 |
|----------------------|-----------------|
| <b>Manuscript ID</b> | [Art. Id: 1327] |
| <b>Author</b>        | C. Chang        |

## AUTHOR:

The following queries have arisen during the editing of your manuscript. Please answer by making the requisite corrections directly in the e-proofing tool rather than marking them up on the PDF. This will ensure that your corrections are incorporated accurately and that your paper is published as quickly as possible.

| Query No. | Nature of Query  |
|-----------|--|
| Q1:       | Your paper has been copy edited. Please review every sentence to ensure that it conveys your intended meaning; if changes are required, please provide further clarification rather than reverting to the original text. Please note that formatting (including hyphenation, Latin words, and any reference citations that might be mistaken for exponents) has been made consistent with our house style. |
| Q2:       | Abstract: Please confirm that the edits to the sentence 'Extensive studies on the....' (and the following sentence) preserve the originally intended meaning.  |
| Q3:       | Please confirm that the edits to the sentence 'In this case,....' preserve the originally intended meaning.  |
| Q4:       | Please note that affiliations have been re-numbered for sequential order.  |
| Q5:       | Please confirm that the edits to the sentence 'In addition, a superionic ....' preserve the originally intended meaning.   |
| Q6:       | Please check your article carefully, coordinate with any co-authors and enter all final edits clearly in the eproof, remembering to save frequently. Once corrections are submitted, we cannot routinely make further changes to the article.  |
| Q7:       | Note that the eproof should be amended in only one browser window at any one time; otherwise changes will be overwritten.  |
| Q8:       | Author surnames have been highlighted. Please check these carefully and adjust if the first name or surname is marked up incorrectly. Note that changes here will affect indexing of your article in public repositories such as PubMed. Also, carefully check the spelling and numbering of all author names and affiliations, and the corresponding email address(es).                                   |
| Q9:       | You cannot alter accepted Supplementary Information files except for critical changes to scientific content. If you do resupply any files, please also provide a brief (but complete) list of changes. If these are not considered scientific changes, any altered Supplementary files will not be used, only the originally accepted version will be published.   |
| Q10:      | If applicable, please ensure that any accession codes and datasets whose DOIs or other identifiers are mentioned in the paper are scheduled for public release as soon as possible, we recommend within a few days of submitting your proof, and update the database record with publication details from this article once available.   |
| Q11:      | Please confirm that the edits to the sentence 'However, the underlying....' preserve the originally intended meaning.  |



# QUERY FORM

| Nature Materials     |                 |
|----------------------|-----------------|
| <b>Manuscript ID</b> | [Art. Id: 1327] |
| <b>Author</b>        | C. Chang        |

## AUTHOR:

The following queries have arisen during the editing of your manuscript. Please answer by making the requisite corrections directly in the e-proofing tool rather than marking them up on the PDF. This will ensure that your corrections are incorporated accurately and that your paper is published as quickly as possible.

| Query No. | Nature of Query  |
|-----------|--|
| Q12:      | Please confirm that the edits to the sentence 'In fact, although current technology....' preserve the originally intended meaning.   |
| Q13:      | Please confirm that the edits to the sentence 'Combining our results....' preserve the originally intended meaning.  |
| Q14:      | Note that journal style reserves the centre dot for the vector dot; please confirm the change to $\times$ in the Maxwell relationship is OK.   |
| Q15:      | Fig. 3: (1) Please confirm the change to the figure title is correct and retains intended meaning. (2) Note that the units have been removed from the log values on the y axes for clarity; the units are described in the text. Please confirm changes are OK.                                      |
| Q16:      | Please confirm that the edits to the sentence 'The finding of the inheritance....' preserve the originally intended meaning.   |
| Q17:      | Fig. 4: (1) title: 'at r.t. (300 K) by MD simulations' - in the Nanoindentation section in Methods, r.t. is given as 293 K. Is this discrepancy correct? (2) Part d, please confirm text added to explain circles is correct. Please add explanation of which colour circle refers to which cluster. |
| Q18:      | Please confirm that the edits to the sentence 'This confirms that....' preserve the originally intended meaning.   |
| Q19:      | Please check the sentence 'The relaxation time....' for clarity. Should this be 'The relaxation time continues to follow the Arrhenius relation for liquid...and its extension overlaps with the experimental...'?   |
| Q20:      | Fig. 5b: note that, as per a previous figure, the units have been removed from the log value on the y axis. Please confirm change is OK  |
| Q21:      | Please confirm that the edits to the sentence 'First, unlike oxide glasses, ....' preserve the originally intended meaning.  |
| Q22:      | Please confirm that the edits to the sentence 'Meanwhile, the time scale of fast....' preserve the originally intended meaning.  |
| Q23:      | Ref. 23: please confirm this is a single-page article/article number or provide page span.   |
|           |  |